tvst

Real-Time Temperature-Controlled Retinal Laser Irradiation in Rabbits

Claus von der Burchard[1], Christopher Kren[2], Jan-Erik Fleger[1], Dirk Theisen-Kunde[2], Veit Danicke[2], Hossam S. Abbas[2,3], Viktoria Kleyman[4], Johann Roider[1], and Ralf Brinkmann[2,5]

[1] Department of Ophthalmology, Christian-Albrechts-University of Kiel, Kiel, Germany
[2] Medical Laser Center Lübeck, Lübeck, Germany
[3] Institute for Electrical Engineering in Medicine, University of Lübeck, Lübeck, Germany
[4] Institute of Automatic Control, Leibniz University Hannover, Hannover, Germany
[5] Institute of Biomedical Optics, University of Lübeck, Lübeck, Germany

Correspondence: Claus von der Burchard, Department of Ophthalmology, Christian-Albrechts-University of Kiel, Arnold-Heller-Straße 3, Kiel 24105, Germany. e-mail: claus.vonderburchard@uksh.de

Purpose: Subdamaging thermal retinal laser therapy has the potential to induce regenerative stimuli in retinal diseases, but validated dosimetry is missing. Real-time optoacoustic temperature determination and control could close this gap. This study investigates a first in vivo application.

Methods: Two iterations of a control module that were optically coupled in between a continuous-wave commercial laser source and a commercial slit lamp were evaluated on chinchilla rabbits. The module allows extraction of the temperature rise in real time and can control the power of the therapy laser such that a predefined temperature rise at the retina is quickly achieved and held constant. Irradiations with aim temperatures from 45°C to 69°C were performed on a diameter of 200 μm and a heating time of 100 ms.

Results: We analyzed 424 temperature-guided irradiations in nine eyes of five rabbits. The mean difference between the measured and aim temperature was -0.04°C $\pm$ 0.98°C. The following ED_{50} values for visibility thresholds could be determined: 58.6°C for funduscopic visibility, 57.7°C for fluorescein angiography, and 57.0°C for OCT. In all measurements, the correlation of tissue effect was higher to the temperature than to the average heating laser power used.

Conclusions: The system was able to reliably perform temperature-guided irradiations, which allowed for better tissue effect control than simple power control. This approach could enhance the accuracy, safety, and reproducibility of thermal stimulating laser therapy.

Translational Relevance: This study is a bridge between preclinical ex vivo experiments and a pilot clinical study.

Introduction

Laser therapies can be used for multiple retinal and macular diseases. Especially for macular diseases, medical therapies have lately widely surpassed laser therapy in number of administrations, but laser therapies still play a prominent role as adjuvant therapy (e.g., in diabetic macular edema [DME] and branch retinal vein occlusion [BRVO]) or as first-line therapy (e.g., in central serous chorioretinopathy [CSCR]). Depending on laser modality and application settings, some collateral morphological and functional damage can arise, which may in some cases be deemed acceptable if overall the functional benefits outweigh the disadvantages. Recent research has focused on laser modalities that can induce a therapeutic effect without any measurable damage, especially photothermal therapies.[1–3]

translational vision science & technology

Photothermal retinal laser therapy relies on absorption of the laser energy mainly by the melanin granula in the retinal pigment epithelium (RPE) and choroid, resulting in a temperature rise and subsequent heat diffusion into adjacent tissues.[4] If the temperature rise stays below the cell damage threshold (coagulation or apoptosis), we refer to that as non-damaging irradiation. These irradiations can be performed by both conventional continuous wave (cw) laser application, as well as by repetitive microsecond pulsed laser application, both of which result in similar heating profiles of the tissue for the same average laser power.[5,6] The non-damaging irradiation spots remain invisible in white light funduscopy, infrared scanning laser ophthalmoscopy, optical coherence tomography (OCT), autofluorescence, and fluorescein angiography (FLA). Therefore, they are also often referred to as "subthreshold" or "subvisible." Nonetheless, there is plenty of evidence that these non-damaging laser therapies can cause multiple favorable tissue effects.[2,3,7,8]

Despite widespread application of these therapies, the therapeutic range or specific temperature increments that will lead to the favorable tissue effects are unknown.[8,9] However, the tissue heating and subsequent effects are only partially correlated to the laser power due to inter- and intraindividual variable light scattering within the whole eye, as well as strong alterations in RPE pigmentation. This likely leads to wide variations in tissue effects among spots with identical irradiation parameters and decreases treatment reliability and reproducibility. Even within the same eye, intraindividual RPE absorption can fluctuate by a factor of 2 to 3,[10] which makes accurate and proper laser power dosing impossible.

Despite these difficulties, some authors assume that the therapeutic range is high enough that a one-size-fits-all therapeutic laser setting can be applied,[11,12] but most studies try to adjust at least for interindividual alterations by applying titration lesions at the vascular arcades to determine the funduscopic visibility threshold and reduce the power by some factor.[2,3,13] However, this still leaves the intraindividual changes in pigmentation not being considered. If the reduction factor is large enough, this titration–lesion-guided approach seems to allow for sufficient safety because coagulation damage becomes improbable. Still, the temperature increase at each location varies approximately proportionally to the absorption (i.e., the density of the local pigmentation), which will result in widely varying temperature profiles across the fundus. Such inhomogeneous temperature spots with unknown temperature increases are unreliable and therefore most likely limited in efficacy.

Our group has previously shown that the temperature rise during retinal laser irradiation can be acquired by optoacoustics,[14] and based on this method we further investigated an automatic real-time temperature control as a possible solution to improve targeting of the therapeutic range.[15–17] This technique has already been used to measure the temperature rise in a clinical study on diabetic macular edema and showed ophthalmoscopically slightly visible damage occurring at temperatures around 65°C to 75°C.[18] Recently, the technology was further improved toward an automatic closed-loop, real-time temperature control with different algorithms.[9,16] The latest approach uses real-time modulation of the treatment laser power with a preset temperature, such that it can be quickly reached and then held for the rest of the irradiation time of 100 ms.[19] The aim of this study was to demonstrate this technique in rabbits and to correlate the thresholds of damage acquired by the different methods with the corresponding temperature rise.

Methods

Laser System, Temperature Measurement, and Real-Time Temperature Control

For temperature-guided irradiation of the retina, a separate optic module for real-time temperature measurement and control was optically coupled in between a conventional 532-nm cw treatment laser (VISULAS 532; Carl Zeiss Meditec, Jena, Germany) and a slit lamp adapted with a laser link (VISULINK 532/U, Carl Zeiss Meditec). Figure 1A provides an overview of the setup. The optics module was equipped with a pulsed 523-nm Q-switched neodymium (Nd):yttrium lithium fluoride (YLF) laser (QL523-500-0; CrystaLaser, Reno, NV) emitting 75-ns pulses with a repetition rate of 3 kHz in order to frequently probe the temperature rise generated by the treatment laser. Both laser beams were modulated with acoustooptical modulators (AOMs; AOM 3080-125 and AOM 3080-1916; Gooch & Housego, Ilminster, UK). The diffracted beams in the first order were superimposed with a dichroic mirror and coupled to a multimode optical fiber (50-μm core, numerical aperture = 0.11; Carl Zeiss Meditec) for transmission to the laser link. The treatment laser is used for tissue heating over a period of 100 ms. The laser pulses are used for repetitively exciting short thermoelastic expansions of pigmented tissue at the fundus, which generate ultrasonic waves with temperature dependent pressure amplitudes. The pressure transients are recorded by an ultrasonic transducer (Medical

Figure 1. (**A**) Schematic layout of the laser system. An optical module is coupled into the fiber between a conventional 532-nm treatment laser and the slit lamp. With optoacoustic feedback recorded by a transducer in the contact glass, a control unit is able to modulate the treatment power in real time to quickly obtain and then constantly hold a preset aim temperature. (**B**) Schematic overview of the temperature profile of a coagulation over time. The measurement pulses in the cooling phase were only applied in the PC system. AOM, acousto-optic modulator; BC, beam collector; BS, beam splitter; PD, photodiode.

Laser Center Lübeck, Lübeck, Germany) embedded in the contact lens and digitized by a data acquisition board.[17,20] A control-unit processes the data in real time to acquire the temperature rise.

To account for the local pigment variations in the RPE and the acoustic coupling, a calibration of the acoustic amplitudes is performed for each individual laser spot. Therefore, the probe laser begins emitting pulses with a pulse energy in the range of 2 to 5 μJ starting 10 ms prior to the cw heating. The measured acoustic amplitudes in the preheating phase are thus referenced to the body temperature of the rabbit.[18]

After starting the heating phase, the rising acoustic amplitudes are converted to the peak tempera-ture and serve as input to a proportional–integral–derivative (PID) controller, which determines the necessary heating power, $P(t)$, to obtain the preset aim temperature rise at the target. The PID therefore sets the voltage applied to the AOM such that the calculated laser power is diffracted into the multimode fiber heading for the laser link. The PID parameters are set such that the aim temperature is reached after about 20 ms and then is held constant for the rest of the overall irradiation time of 100 ms (see Fig. 1B).

During the development of the PID controller, two iterations were realized: The first iteration was a PC-based system with self-written control software written in C, in combination with a dual-channel

PCIe digitizer card with an input bandwidth of 100 MHz and a sample rate of 100 megasamples (MS)/s. Signal conditioning of the optoacoustic transients gathered from the contact glass was performed by a series connection of two external amplifiers—Olympus 5660B Ultrasonic Preamplifier (60 dB; Olympus, Tokyo, Japan) and SRS SR560 (10×; Stanford Research Systems, Sunnyvale, CA)—and an amplifier–internal bandpass filter ($F_L = 10$ kHz, $F_H = 1$ MHz). This system was used to test the performance of various parameter sets of the PID controller. Details and the control architecture are described in detail by Herzog et al.[19] With this device, the first part of this study was conducted on rabbits.

After successful testing, the design of the controller was transferred into a fully integrated stand-alone microcontroller module. Real-time signal processing, controlling, and system monitoring were performed by a processor board developed for this purpose (hardware by Lacon Electronic GmbH, Karlsfeld, Germany; software by Curefab Technologies, Munich, Germany). The controller architecture and the PID parameter were identical to the best performing set on the PC system. In contrast to the PC module, no further measurement pulses were applied after the 100-ms heating phase to monitor the cooling phase. This was intended to apply less energy in future use in a clinical study. Also, whereas the PC system used a preset individually chosen pulse energy to achieve a sufficiently high signal-to-noise ratio, the microcontroller system used three energy settings to test the signal-to-noise ratio achieved by the respective pulse energy during calibration phase. The lowest level with sufficient signal quality was used in the subsequent heating phase. The optoacoustic transients measured with the contact glass were amplified and filtered by a preamplifier integrated in the transducer(40 dB) and a downstream post-amplifier (40 dB) with an integrated bandpass filter ($F_L = 800$ kHz, $F_H = 1.2$ MHz). Additionally, another high-pass filter (40 kHz) and low-pass filter (1.5 MHz) were applied at the signal input of the controller board. With this device, the second part of this study on rabbits was conducted to confirm the results of the first study and to prepare for the clinical trial.

The acoustic transients are emitted from the whole irradiated and pigmented volume (mainly the RPE and choroid); thus, their amplitudes refer to the average temperature rise, $\Delta T_{OA}(t)$, over this volume. Of most interest with respect to cellular effects and thermal damage is the highest temperature in the irradiated volume, $\Delta T_{peak}(t)$, which is obtained in the center of the beam within the RPE. In order to extract this peak temperature from the measured average temperature, $\Delta T_{OA}(t)$, a time-dependent conversion function, $f(t)$, is applied according to

$$\Delta T_{peak}(t) = f(t) \times \Delta T_{OA}(t)$$

Details are describes by Brinkmann et al.[18] For a 200-µm² spot and a typical temperature course, $\Delta T_{OA}(t)$, achieved with a course $P(t), f(t)$ can be calculated mathematically and approximated by exponential functions.

This paper analyzes data obtained with both systems. The conversion function used in the PC system was taken over to the microcontroller device. However, later analysis showed that the fast temperature rise followed by a constantly held temperature was not adequately modeled with the conversion function, which had been modeled for a constant laser power. Therefore, the conversion function was adapted to the temperature profile caused by power modulation in the microcontroller system (see Supplementary Fig. S1). Due to this fact, the temperatures determined with the microcontroller device were systematically lower by about 2°C. Because these measurements were used for the PID, we continued using these measurements for the determination of accuracy of the control mechanisms (Figs. 2–4). To better determine the median effective dose (ED_{50}) values for both treatment series, for ED_{50} analysis, the temperatures were afterwards recalculated with the appropriate conversion function for the PC system, so that all of the temperatures were comparable (Fig. 5).

Animal Experiments on Rabbits In Vivo

The experiments on rabbits in vivo were carried out according to German law for the protection of animals, approved by the Ministry of Energy Transformation, Agriculture, Environment, Nature and Digitalization of Schleswig-Holstein, Kiel, Germany (V242-68848/2019). The experiments adhered to the ARVO Statement for the Use of Animals in Ophthalmic and Vision Research. The rabbits were anesthetized before the measurement with a MMF narcosis (medetomidine, 0.2 mg/kg body weight; midazolam, 1 mg/kg body weight; fentanyl, 20 µg/kg body weight) applied subcutaneously. They were fixed in a special holding device and positioned in front of the slit lamp. Phenylephrine (2.5%) and tropicamide (0.5%) eye drops were used to dilate the pupils, and oxybuprocaine (0.4%) eye drops were used for local anesthesia of the cornea. The modified contact lens was fixed onto the rabbit's cornea using a custom holder. Hypromellose gel (2%) was used as a contact agent for optical and acoustical coupling of the contact lens and cornea. Body temperature was measured rectally before treatment for
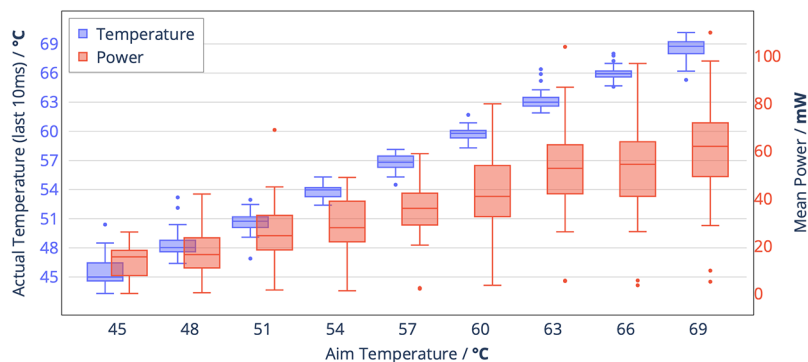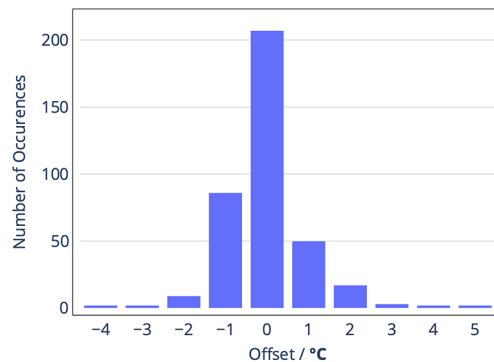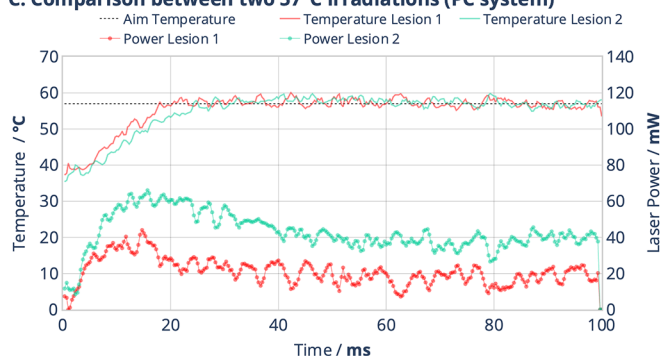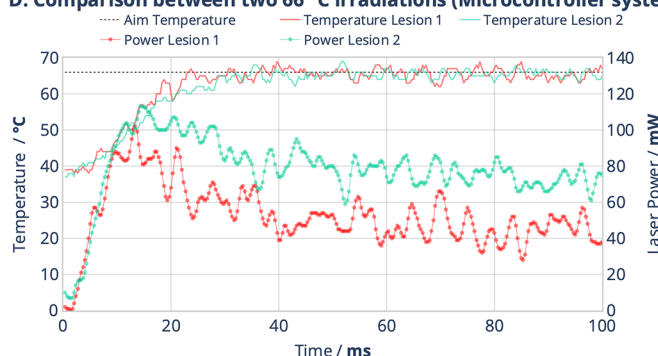
Figure 2. Accuracy of the system. (**A**) Box plot of aim temperature versus achieved temperature and mean applied power. (**B**) Bar graph of temperature offset. (**C**, **D**) For the PC and microcontroller systems, two exemplary irradiations are shown with very similar temperature profiles in the same rabbit. In both systems, the temperature curves are almost identical, but it can be shown that the mean applied power to reach the temperature differs by factors of 2.0 (PC system) and 1.5 (microcontroller system) for these exemplary irradiations.

baseline temperature calibration and during the experiments for surveillance.

After all of the experimental procedures were completed, the narcosis was ended via an antidote (atipamezole, 1 mg/kg body weight; flumazenil, 0.1 mg/kg body weight; naloxone, 30 µg/kg body weight).

Irradiation Protocol

One eye was treated per session. The contact lens was placed so that the optic disc and the band of medullated nerve fibers were at the top of the visible fundus area. Then, suprathreshold marker lesions with 300-µm^2 diameter were set as boundaries for roughly 2×2-mm treatment areas. In each area, nine spots, 200 µm^2/100 ms, were irradiated with ascending aim temperatures from 45°C to 69°C in 3°C steps (see Fig. 3). Per rabbit, on average six of these treatment areas were irradiated. We chose this setup to distribute all aim temperatures homogeneously over the whole fundus so that a possible influence of central versus peripheral location would have also been distributed equally.

Imaging and Image Analysis

One hour after completion of treatment irradiation, retinal imaging was performed. We first obtained densely sampled OCT volume scans (SPECTRALIS HRA+OCT2; Heidelberg Engineering, Heidelberg, Germany) and then performed color fundus photography and FLA with the ZEISS VISUCAM. For FLA, about 0.2 mL of 10% fluorescein (Alcon, Geneva, Switzerland) was inserted into an ear vein of the rabbit.

All image data were later reviewed by author J.F. in order to classify funduscopic and FLA visibility in a binary yes/no fashion. On OCT data, the greatest linear diameter (GLD) was measured with the proprietary software of the device. The definite (if visible in infrared image) or otherwise supposed irradiation site of each treatment lesion was thoroughly inspected for clearly demarked or highly suggestive alteration in the RPE or photoreceptor layer. If alterations were found, the B-scan over the lesion with the largest horizontal diameter was chosen, and the
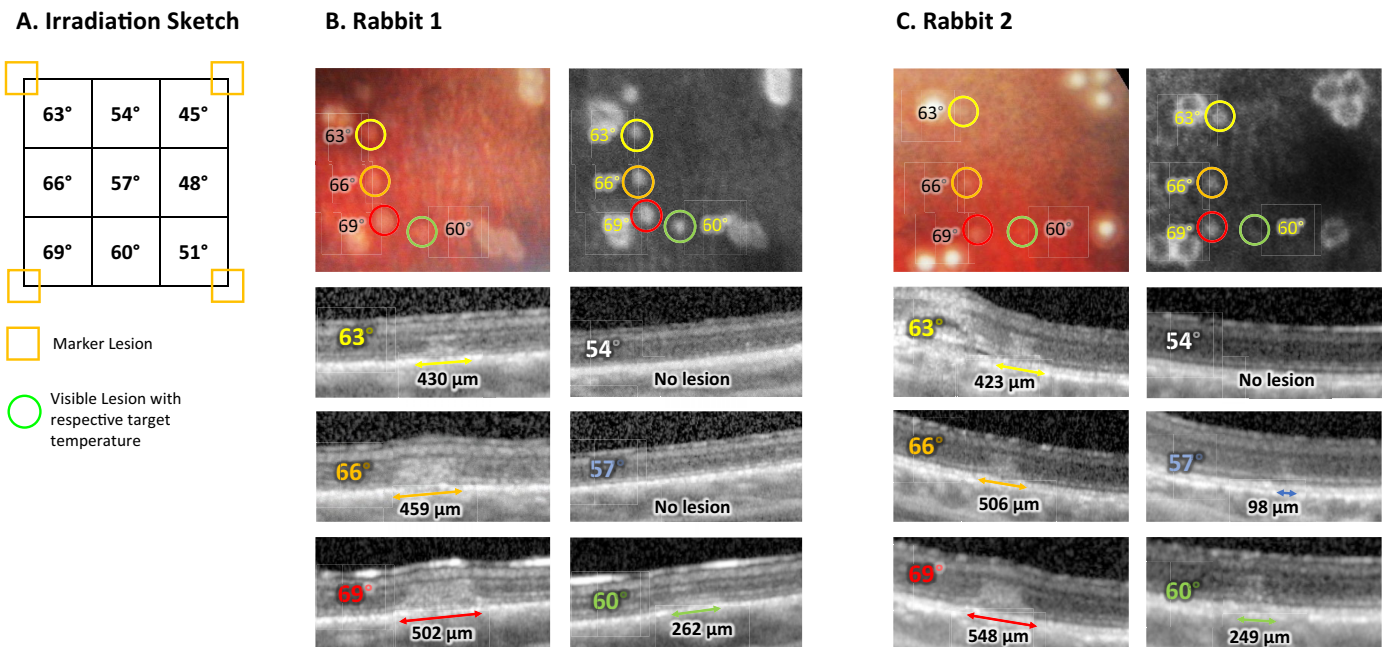
Figure 3. (**A**) The fundus was divided into different irradiation areas by high-intensity marker lesions. In each area, nine irradiations with ascending aim temperatures from 45°C to 69°C in steps of 3°C were performed. (**B**, **C**) Two exemplary irradiation sites in FLA and color fundus photography. For each lesion between 54° and 69°C, the corresponding OCT with GLD measurement is shown. Notice that around the ED_{50} mark of 57°C some but not all lesions were detectable in OCT.

Statistical Analysis and Illustrations

Statistical analysis was performed in Python. Correlations between temperature and tissue effect (Fig. 4) were determined by fitting an exponential curve with the scipy package. Graphics were created with the plotly library. ED_{50} values were calculated and visualized with a probit function in R (R Foundation for Statistical Computing, Vienna, Austria) and the ggplot2 library. To determine the coefficient of determination for ED_{50} plots, a pseudo-R^2 value, $R^{2}*$, was calculated with the method described by McFadden.[21] The standard error of the mean for a sample size N with a standard deviation σ was defined as $\sigma/\sqrt{N}$.

Results

Accuracy of Temperature Control

For the PC-based system, 186 lesions in four eyes of two rabbits were analyzed. For the microcontroller-based system, 238 lesions in five eyes of three rabbits were analyzed. The mean difference between the measured temperature (within the last 10 ms) and the aim temperature was $-0.04°C \pm 0.98°C$, and the standard error of the mean was 0.05°C; 95.6% of lesions were within $\pm 2°C$ (Fig. 1B). Figure 1A shows that the mean applied power to reach and hold the temperature varied much more greatly than the actual measured temperature, which emphasizes the necessity of real-time power modulation for temperature-guided laser coagulation. Figures 1C and 1D show exemplary time courses for the PC and microcontroller system, each showing two exemplary lesions with a similar temperature profile (continuous lines, top), but different power profiles (dotted lines, bottom).

Correlation of Temperature to Tissue Effect

For both systems, we correlated the temperature (and respective applied power) to the resulting tissue defect. Figure 3 shows exemplary lesions that indicate that the tissue effect correlated well to the preset aim temperature. To correlate lesion strength to the preset aim temperature, to the actual temperature during the last 10 ms of coagulation, and to the average applied power, we chose GLD in OCT as a lesion strength surrogate. GLD offers the advantage that it can be better quantified than funduscopic or FLA visibility, as shown in Figure 3C. It could be shown that the lesion
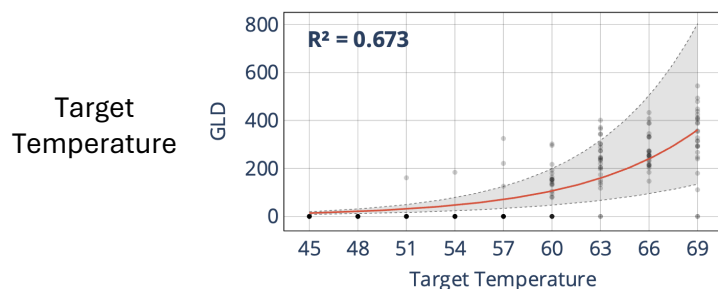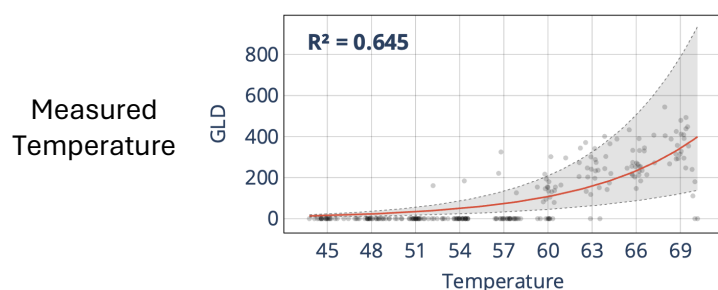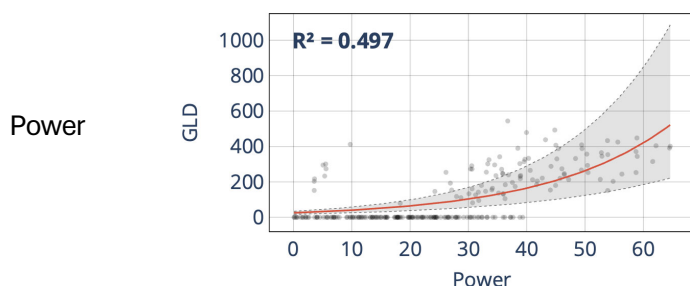
PC System   Microcontroller System
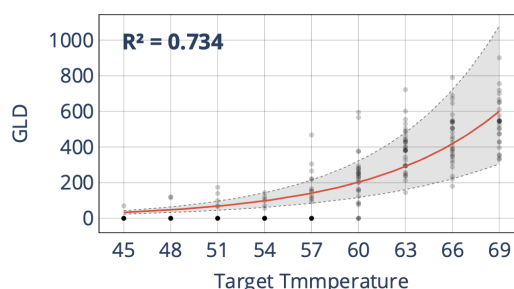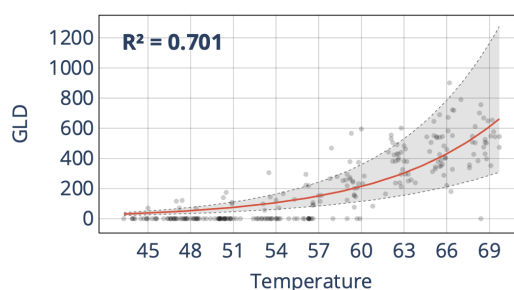
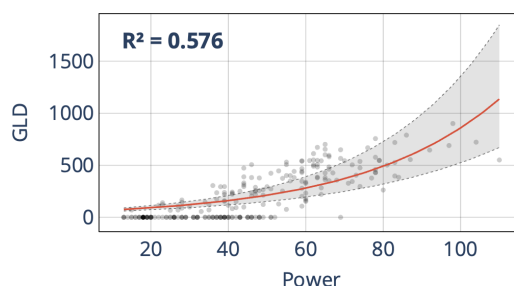**Figure 4.** Correlation of OCT GLD to aim temperature, measured temperature, and power.

strength correlates much better to the aim temperature ($R^2 = 0.673$ for the PC system and $R^2 = 0.734$ for the microcontroller system) and actual measured temperature during the last 10 ms of the irradiation ($R^2 = 0.645$ and $R^2 = 0.701$, respectively) than to the averaged power during the coagulation ($R^2 = 0.497$ and $R^2 = 0.576$, respectively) (see Fig. 4).

Because both systems performed with comparable accuracy, determination of the ED_{50} was performed in a pooled analysis to increase sample size. We were able to determine the following ED_{50} values:

- For funduscopic visibility after 1 hour, $ED_{50} = 58.6°C$ (95% confidence interval [CI], 57.8–59.5;

$R^2* = 0.51$; PC system, 59.4°C; microcontroller, 58.5°C)
- For fluorescein angiography visibility after 1 hour, $ED_{50} = 57.7°C$ (95% CI, 56.9–58.4; $R^2* = 0.58$; PC system, 58.1°C; microcontroller, 57.2°C)
- For OCT visibility after 1 hour, $ED_{50} = 57.0°C$ (95% CI, 56.3–57.7; $R^2* = 0.66$; PC system, 57.7°C; microcontroller, 56.2°C).

Again, the correlation was much higher for temperature ED_{50} calculations than for correlation to power (see Fig. 5). A difference of $\leq 1.5°C$ for all ED_{50} measurements between the two systems further indicates the robustness of the system.
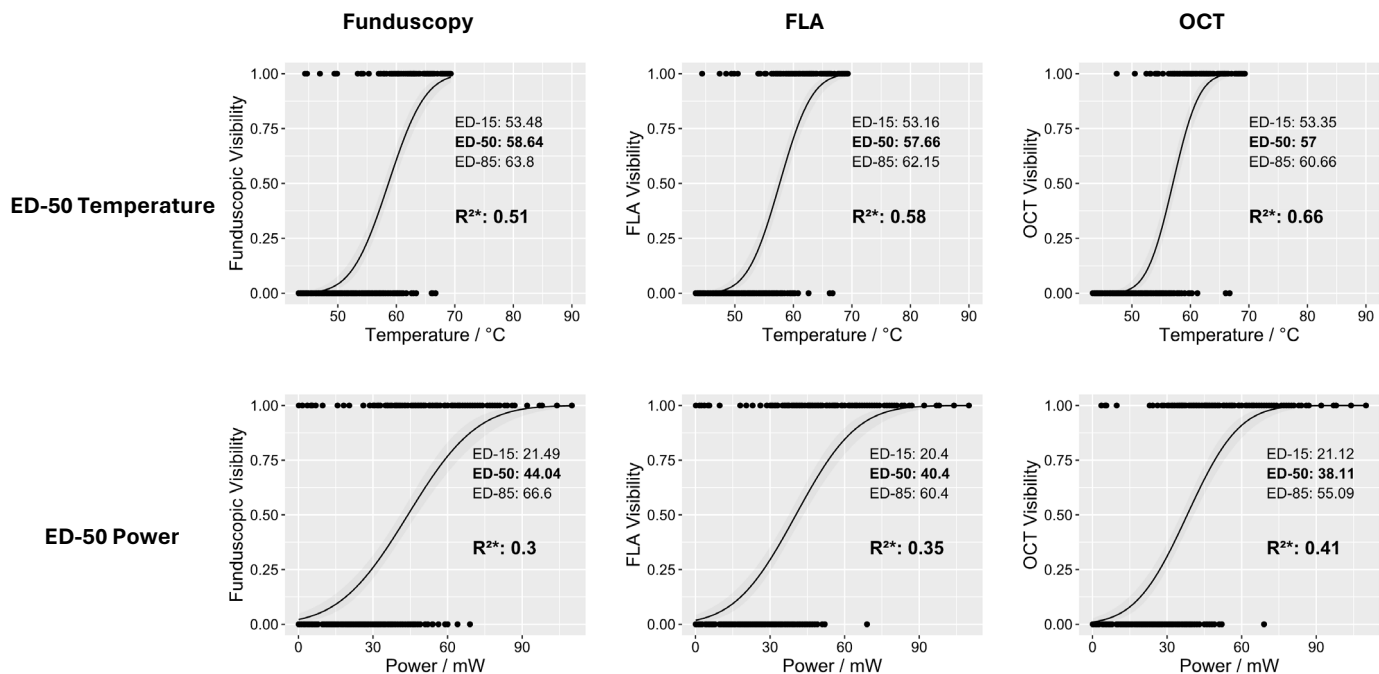
Figure 5. ED_{50} determination via probit plot method (pooled analysis for PC and microcontroller systems).

Discussion

The aim of this new temperature-guided retinal laser treatment is to provide a reliable temperature increase for retinal thermal stimulation without inducing any adverse effects such as tissue coagulation or induction of apoptosis. None of the current titration techniques (e.g., probe irradiation at the arcades) provides sufficient accuracy due to the large pigmentation and thus absorption differences across the individual fundi. The technique demonstrated here allows the temperatures to rise equally for each single irradiation spot. The desired temperature rise can be chosen freely prior to the irradiation, and the technique will automatically adjust for this. The implemented closed-loop technique investigated in thus study (with two different implementations) is the first application in vivo on rabbits. Apart from this optoacoustic method, no other non-invasive technology exists to validate a retinal temperature rise over an irradiation period as short as 100 ms in a living eye. Real-time temperature readout via electroretinogram has been proposed but only works for much longer irradiation times.[22] Other researchers have proposed the use of real-time OCT for dosimetry[23]; however, measurable OCT alterations are mainly expected above the coagulation threshold, which limits usability. In ex vivo experiments, real-time OCT detection of subvisible lesions has been reported[24]; however, data are limited with regard to the accuracy of these measurements and if the sensitivity allows for reliable dosimetry.

Evolution of Temperature-Guided Retinal Irradiation

Our research group has previously reported on temperature-guided retinal photocoagulation with optoacoustic feedback. Koinzer et al.[15,20] established a fixed-power variable-time approach, where a constant irradiation power was held until the desired aim temperature was reached. This was a first step toward more reproducible and uniform lesion strengths based on the Arrhenius damage integral accounting for the temperature and time of elevated temperature. However, in a clinical setting, widely varying irradiation times can be seen as impractical and especially longer irradiation times are more susceptible to motion artifacts.

Baade et al.[17] demonstrated a fixed-time variable-power approach, where the overall 50-ms irradiation time was split into a calibration phase of 10 ms and two 20-ms treatment phases with constant power levels: first for 20-ms absorption probing with a predefined power and, second, for another 20 ms of heating

toward the desired aim temperature. The power needed to achieve the aim temperature was increased proportionally to the probing temperature. Despite overall reaching the desired aim temperature with reasonable accuracy, the standard deviation of the temperature offset varied from 2.1°C for 50°C irradiations up to 5.0°C for 70°C irradiations, which is much higher than the 0.98°C found in our study (for all temperatures). Because the power was only modulated one time, the system was especially prone in cases where only a little temperature rise occurred during the probing phase. By using a real-time feedback loop, our system showed much better reliability in these situations. The reported ED_{50} value of 65.3°C for funduscopic visibility is slightly higher than in our study, as can be expected without the long plateau phase where the aim temperature is held constant.

Both previous iterations of temperature-guided photocoagulation required hardware modification of the treatment laser. The setup investigated in this study uses a separate optics module that can modify a fixed power output of a shelf commercial laser system and apply the power to a commercial laser application device such as a slit lamp. This has multiple advantages: First, it is independent of the model of the input laser (i.e., is manufacturer independent and independent of software/hardware maintenance). Second, because the laser interferes with neither the input laser nor the output slit lamp, regulatory approval affects only the optics module. Third, the module can only dampen but never increase the input laser power, which allows for a considerable security increase: If the input power is set reasonably low (for example, around the expected funduscopic visibility threshold), then the system can never exceed this input power. Thereby, even in case of completely faulty temperature measurements, excessive irradiation strength is ruled out.

Proof of Effectiveness

The above-mentioned previous studies have shown that time and power modulation can be used to reach a predefined aim temperature. It has also been shown that temperature-guided photocoagulation can be used to create uniform lesions with different input settings.[25] However, it had not conclusively been proven in clinical studies that this approach is advantageous over classic power titration. Therefore, we used the probit and correlation analysis to demonstrate that tissue effect correlates better to temperature than to power (Figs. 4, 5). Both analyses underline our hypothesis that temperature-guided retinal coagulation can also improve lesion reproducibility when aiming for temperatures above the coagulation threshold. The findings

furthermore support the validity of the temperature measurements. Moreover, the equally good correlation of tissue effect to the aim temperature as to the achieved temperature (Fig. 4) illustrates the reliability of the temperature modulation. Because light scattering and fundus pigmentation vary among different animals, it might be argued that pooling different eyes might be illegitimate for power analysis; importantly, however, the correlation in both probit and exponential regression analysis was also better when analyzing individual eyes (data not shown due to abundancy).

For all analysis in tissue effect, it must be considered that the accuracy of the diagnostic imaging is limited. Especially for color fundus photography and FLA, the system used for imaging was chosen because of its availability for animal studies rather than for excellence in imaging quality. Further, because the system was designed for human use, imaging was complicated and quality impaired. This limited accuracy can at least partially explain why the R^2 coefficients are still well below 1.

OCT proved to be the most reliable imaging system, even though the OCT system was designed for in-human use and the image quality was reduced because the rabbit eye could not ideally be installed on the head rest of the system. When determining OCT visibility, we checked for any ever so small alteration around the irradiation site. This very sensitive approach was chosen to detect all irradiation damage; however, in some cases with only small variations in the ellipsoid zone of the photoreceptors, it remains questionable whether this really was laser induced or rather an imaging artifact. This might explain why in a few outliers, even in very low temperature and power ranges, OCT visibility was diagnosed.

Implications on Future Retinal Laser Therapy

Except for very few opposing views,[11,12] the need for appropriate dosing in retinal laser therapy is generally agreed upon. As Figure 5 shows, the laser power alone can only partially explain the tissue effect. Most likely the intraindividual pigmentation alterations[10] play a major role. Unfortunately, this cannot be accounted for with traditional dosing strategies in the form of titration lesions, which only corrects for interindividual variations.

A review of subthreshold microsecond pulsed laser for macular diseases found staggering variations among the different studies, with visual acuity gains ranging from −15 to +20 letters for CSCR, −7 to +19 for DME, and −4 to +10 for BRVO.[26] Although small sample sizes, heterogeneous study populations, and different treatment patterns, among

other factors, probably account for most of these fluctuations, it might be hypothesized that imprecise targeting of the therapeutic range also played a role. Because of the similar temperature profiles and damage ranges between microsecond pulsed and continuous wave lasers when applying the same average power,[5,6] similarly imprecise results can also be expected for other thermal subvisible laser therapies. It seems reasonable that, with more reliable targeting of the therapeutic effect, more consistent data could be acquired in both clinical studies and real life.

Especially in CSCR, where no medical treatment has been proven beneficial, laser therapies are still first-line therapy, and any means to improve therapy results is urgently needed. Additionally, with the recent worldwide shortage of verteporfin, thermal laser therapies have become the only remaining therapeutic option in many CSCR cases. Therefore, we also chose CSCR as the clinical condition for a pilot study that we are currently conducting.[27,28]

In preclinical studies, thermal stimulation of the retina has also shown therapeutic potential for other diseases such as intermediate AMD,[3,7] where as of today no established therapy exists. Intermediate AMD, however, is often only associated with little subjective visual impairment. Early prophylactic thermal treatment of such eyes would call for even higher safety profiles. We think that temperature-guided laser therapy might help to favorably improve the safety profile in such cases.

Also for above-threshold, visible laser therapy, temperature-guided laser therapy can be beneficial. In ischemic diseases such as diabetic retinopathy or retinal vein occlusion, destruction of tissue with sufficient laser power still is the mainstay of therapy. However, the higher the power, the deeper and stronger are the lesions and the more pain is inflicted upon patients, which especially in cases of overtreatment can be extensively bothersome for the patients. Therefore, an efficient targeting of the coagulation strength in order to prevent unnecessary overtreatment could be an interesting option in future therapies.

Limitations

It must be considered that the accuracy of the temperature measurement is limited by the Grüneisen coefficient of retinal tissue, which is used for calibration. Even though data from rabbit, pig, and sheep eyes with retinal tissue similar to that of humans achieve the same values, the coefficient for human eyes, especially for pathologic sites, is not known. However, because mainly the RPE and choroidal pigmentation account for the thermoelastic response, it might

be hypothesized that this error is small. Further, the system was used in anesthetized rabbits. In human use, involuntary eye and head movements as well as movements of the contact glass by the operator might be a source of error. This, however, can easily be detected as a sudden, unexpected change in temperature profile. In such cases, the module could immediately stop the irradiation. In the future, model predictive control algorithms, compared to the PID control used here, could further reduce inaccuracies due to the conversion function by real-time parameter estimation.[29–31]

In our study, we have only investigated the real-time temperature control setup with a cw laser. It previously has been shown that the optoacoustic temperature measurement can also be used in comparison with microsecond pulsed lasers.[5] Therefore, it can be assumed that a real-time control algorithm could be implemented in combination with a microsecond pulsed laser in a comparable fashion. However, future studies are needed to confirm this assumption.

Conclusions

The results of this first, to our knowledge, in vivo study demonstrate that a temperature-guided automatic control was able to achieve reproducible and reliable real-time temperature-controlled irradiation. The power control module reliably allows achieving preset aim temperatures in the non-damaging range, which makes it an ideal tool for uniform but subvisible irradiations. When using aim temperatures above the coagulation threshold, temperatures correlated better to the damage size than to the laser power. In the long term, this technology has great potential to achieve more consistent and better results than conventional laser methods in conjunction with titration spots outside the target area, especially for subdamaging effects.

Acknowledgments

Disclosure: **C. von der Burchard**, None; **C. Kren**, None; **J.-E. Fleger**, None; **D. Theisen-Kunde**, None; **V. Danicke**, None; **H.S Abbas**, None; **V. Kleyman**, None; **J. Roider**, None; **R. Brinkmann**, Medizinisches Laserzentrum Lübeck (P)

References

1. Chhablani J, Roh YJ, Jobling AI, et al. Restorative retinal laser therapy: present state and future directions. *Surv Ophthalmol*. 2018;63(3):307–328.

2. Lavinsky D, Sramek C, Wang J, et al. Subvisible retinal laser therapy: titration algorithm and tissue response. *Retina*. 2014;34(1):87–97.

3. Tode J, Richert E, Koinzer S, et al. Thermal stimulation of the retina reduces Bruch's membrane thickness in age related macular degeneration mouse models. *Transl Vis Sci Technol*. 2018;7(3):2.

4. Birngruber R, Hillenkamp F, Gabel VP. Theoretical investigations of laser thermal retinal injury. *Health Phys*. 1985;48(6):781–796.

5. Miura Y, Inagaki K, Hutfilz A, et al. Temperature increase and damage extent at retinal pigment epithelium compared between continuous wave and micropulse laser application. *Life (Basel)*. 2022;12(9):1313.

6. Wang J, Quan Y, Dalal R, Palanker D. Comparison of continuous-wave and micropulse modulation in retinal laser therapy. *Invest Ophthalmol Vis Sci*. 2017;58(11):4722–4732.

7. Richert E, von der Burchard C, Klettner A, et al. Modulation of inflammatory processes by thermal stimulating and RPE regenerative laser therapies in age related macular degeneration mouse models. *Cytokine X*. 2020;2(3):100031.

8. Sramek C, Mackanos M, Spitler R, et al. Non-damaging retinal phototherapy: dynamic range of heat shock protein expression. *Invest Ophthalmol Vis Sci*. 2011;52(3):1780–1787.

9. Baade A, von der Burchard C, Lawin M, et al. Power-controlled temperature guided retinal laser therapy. *J Biomed Opt*. 2017;22(11):1–11.

10. Lappin PW, Coogan PS. Relative sensitivity of various areas of the retina to laser radiation. *Arch Ophthalmol*. 1970;84(3):350–354.

11. Luttrull JK. Low-intensity/high-density subthreshold diode micropulse laser for central serous chorioretinopathy. *Retina*. 2016;36(9):1658–1663.

12. Moisseiev E, Abbassi S, Thinda S, Yoon J, Yiu G, Morse LS. Subthreshold micropulse laser reduces anti-VEGF injection burden in patients with diabetic macular edema. *Eur J Ophthalmol*. 2018;28(1):68–73.

13. van Dijk EHC, Fauser S, Breukink MB, et al. Half-dose photodynamic therapy versus high-density subthreshold micropulse laser treatment in patients with chronic central serous chorioretinopathy: the PLACE trial. *Ophthalmology*. 2018;125(10):1547–1555.

14. Kandulla J, Elsner H, Birngruber R, Brinkmann R. Noninvasive optoacoustic online retinal temperature determination during continuous-wave laser irradiation. *J Biomed Opt*. 2006;11(4):041111.

15. Koinzer S, Schlott K, Ptaszynski L, et al. Temperature-controlled retinal photocoagulation —a step toward automated laser treatment. *Invest Ophthalmol Vis Sci*. 2012;53(7):3605–3614.

16. Schlott K, Koinzer S, Ptaszynski L, et al. Automatic temperature controlled retinal photocoagulation. *J Biomed Opt*. 2012;17(6):061223.

17. Baade A, von der Burchard C, Lawin M, et al. Power-controlled temperature guided retinal laser therapy. *J Biomed Opt*. 2017;22(11):1–11.

18. Brinkmann R, Koinzer S, Schlott K, et al. Real-time temperature determination during retinal photocoagulation on patients. *J Biomed Opt*. 2012;17(6):061219.

19. Herzog C, Thomsen O, Schmarbeck B, Siebert M, Brinkmann R. Temperature-controlled laser therapy of the retina via robust adaptive H_∞-control. *Automatisierungstechnik*. 2018;66(12):1051–1063.

20. Schlott K, Koinzer S, Baade A, Birngruber R, Roider J, Brinkman R. Lesion strength control by automatic temperature guided retinal photocoagulation. *J Biomed Opt*. 2016;21(9):98001.

21. McFadden D. Conditional logit analysis of qualitative choice behavior. In: Zarembka P, ed. *Frontiers in Econometrics*. Cambridge, MA: Academic Press; 1974:105–142.

22. Kaikkonen O, Turunen TT, Meller A, Ahlgren J, Koskelainen A. Retinal temperature determination based on photopic porcine electroretinogram. *IEEE Trans Biomed Eng*. 2022;69(2):991–1002.

23. Müller HH, Ptaszynski L, Schlott K, et al. Imaging thermal expansion and retinal tissue changes during photocoagulation by high speed OCT. *Biomed Opt Express*. 2012;3(5):1025–1046.

24. Veritti D, Sarao V, Lanzetta P. Online optical coherence tomography during subthreshold laser irradiation. *Eur J Ophthalmol*. 2012;22(4):575–579.

25. Koinzer S, Baade A, Schlott K, et al. Temperature-controlled retinal photocoagulation reliably generates uniform subvisible, mild, or moderate lesions. *Transl Vis Sci Technol*. 2015;4(5):9.

26. Scholz P, Altay L, Fauser S. A Review of subthreshold micropulse laser for treatment of macular disorders. *Adv Ther*. 2017;34(7):1528–1555.

27. Theisen-Kunde D, von der Burchard C, Danicke V, et al. Real-time temperature-control

for cw retinal laser therapy in a clinical study. In: *Translational Biophotonics: Diagnostics and Therapeutics III* (Vol 12627). Bellingham, WA: SPIE; 2023:195–199.

28. von der Burchard C, Danicke V, Kren C, et al. Real-time temperature-guided laser therapy in central serous chorioretinopathy. *Invest Ophthalmol Vis Sci*. 2023;64(8):1806.

29. Kleyman V, Schaller M, Mordmuller M, et al. State and parameter estimation for retinal laser treatment. *arXiv*. 2022, https://doi.org/10.48550/arXiv.2203.12452.

30. Schaller M, Wilson M, Kleyman V, et al. Parameter estimation and model reduction for model predictive control in retinal laser treatment. *Control Eng Pract*. 2022;128:105320.

31. Schaller M, Kleyman V, Mordmüller M, et al. Model predictive control for retinal laser treatment at 1 kHz. *Automatisierungstechnik*. 2022;70(11):992–1002.